Interfacial behavior of randomly charged sulfonated polystyrene (PSS) at the air/water interface

Young-Soo Seo [a], Farhan Ahmad [b], Kwanwoo Shin [c,*], Ju-Myung Song [d], Joon-Seop Kim [d], Miriam H. Rafailovich [e], Jon Sokolov [e], Sushil K. Satija [f]

[a] *Department of Nano Science and Technology, Sejong University, Seoul 143-747, Republic of Korea*
[b] *Department of Materials Science and Engineering, Gwangju Institute of Science and Technology, Gwangju 500-712, Republic of Korea*
[c] *Department of Chemistry and Program of Integrated Biotechnology, Sogang University, Seoul 121-742, Republic of Korea*
[d] *Department of Polymer Science and Engineering, BK21 Education Center of Technology for Advanced Materials and Parts,*
Chosun University, Republic of Korea
[e] *Department of Materials Science and Engineering, Stony Brook University, Stony Brook, NY 11794, United States*
[f] *National Institute of Standards and Technology, Gaithersburg, MD 20899, United States*

Abstract

Langmuir monolayers of randomly charged polystyrene sulfonated acid, PSS_x, with various degrees of sulfonation (x) ranging from 4 up to 35% were studied. Three characteristic regimes of PSS_x were determined, according to the balance between electrostatic and hydrophobic interactions in these ranges. Low charged PSS (4–5%) aggregates to irreversible films upon compression, leading to strong hysteresis. Moderately charged PSS (6–16%) is shown to less hysteretic. In contrast, highly charged PSS (35%) formed a reversible film due to dominant electrostatic interactions over hydrophobic interaction. Using in situ neutron reflectivity (NR) we observed that PSS with 35% sulfonation formed a highly stretched brush into the water subphase upon compression.
© 2007 Elsevier B.V. All rights reserved.

Keywords: Polyelectrolytes; Langmuir monolayer; Polystyrene sulfonated acid

1. Introduction

A sound understanding of the interfacial behavior of polyelectrolytes is necessary for numerous applications in thin film coating technology, particularly those involving biomimetic membranes [1,2], stabilization of colloids [3], electronic materials [4,5], and cell adhesion for biomedical applications [6,7]. A variety of external parameters, such as salt concentration [8,9], pH [10–12] and temperature [13] of the subphase and the nature of the adsorbing surface [14,15] are important for controlling and tuning the interfacial properties of polyelectrolytes. The adsorption characteristics of polyelectrolytes on various surfaces have been reported [4,5,16,17]. Especially, an air/water [18,19] interface has been widely chosen due to its neutrality, smoothness and strong surface attraction to polymers.

Adsorption of highly charged polyelectrolytes at air/water interface has been extensively studied by Yim et al. [20], where chain conformations of PSS_{90} are dependent upon molecular weight and salt concentration. They observed that the adsorbed layer formed a bilayer profile comprising a 10–20 Å thick dense layer at the air surface followed by loosely extended layer (i.e., brush-like conformation) into the water. In the presence of a high salt concentration, the extended layer thickness increased due to the screening of the electrostatic charge on the chain. Behavior of less charged PSS has also been studied by Theodoly et al. [21] with a degree of sulfonation between 30 and 90%, where they found that rate of adsorption was very slow, partially irreversible, and strongly hysteretic.

The goal of this research is to understand detailed conformation of randomly charged polystyrene sulfonic acid (PSS_x) with degrees of sulfonation (x) ranging from 4 to 35% at the air/water interface. The interfacial behavior of lower charged polymers would be strongly influenced by hydrophobic interactions, while highly charged polymers act very differently, indicative of strong

* Corresponding author. Tel.: +82 2 705 8441; fax: +82 2 715 0797.
E-mail address: kwshin@sogang.ac.kr (K. Shin).

charge repulsion, causing less hysteresis and brush formation. We examined the phase isotherm, hysteresis, and conformations of the adsorbed monolayer using the Langmuir balance technique as well as in situ neutron reflectivity (NR) measurements. From surface pressure–area analysis of Langmuir monolayer, we were able to categorize these polyelectrolytes into three different regimes, i.e., *hydrophobic*, *ionomer*, and *polyelectrolyte* regimes as a function of the degree of sulfonation. For the first time, we were able to observe the reversible contraction and stretching of polyelectrolytes with ionic contents $x \geq 35\%$ at the air/water interface using in situ NR measurement. By varying the charge contents on the hydrophobic polystyrene from 4 to 35%, we were able to provide experimental evidence, quantifying the transition from dense/hysteretic to expanded/reversible with increasing sulfonation, and the conditions for the submersion of strands.

2. Experiment

2.1. Materials

Polystyrene was prepared by bulk free radical polymerization. Poly(*styrene-ran*-styrenesulfonic acid) (PSS) with a various degree of sulfonation ranging from 4 to 35% was prepared by the sulfonation method developed by Makowski et al. [22]. Deuterated PSS with 9 and 35% sulfonation were also synthesized for use in neutron reflectivity studies. The complete specifications of the samples are listed in Table 1.

2.2. Langmuir monolayer

Surface pressure (π)–area (A) isotherms were recorded at a compression rate of 10 mm/min using a KSV 2000 Langmuir trough with two computer-controlled moving barriers. The total area of the Langmuir trough was 772.5 cm^2, and it was placed within a Plexiglass box. The Langmuir trough was placed on an anti-vibration optical table. A 25 mm wide platinum Wilhelmy plate, suspended from a microbalance, was used to monitor the surface pressure. The Wilhelmy plate was properly cleaned by a high temperature treatment. Water with a resistivity of 18 MΩ cm, was used as the subphase. The temperature was maintained at room temperature (∼22 °C) using an external water chiller.

Table 1
Characterization of the polystyrene sulfonated acids (PSS$_x$) used in this study

Designation	x [mol%]	M_w [g/mol]
h-PSS$_4$	4.0	110 k
h-PSS$_5$	5.0	100 k
h-PSS$_6$	6.0	150 k
d-PSS$_9$[a]	9.0	169 k
h-PSS$_{11}$	11.0	150 k
h-PSS$_{14}$	14.0	300 k
h-PSS$_{16}$	16.0	150 k
d-PSS$_{35}$[a]	35.0	252 k

[a] d-PSS$_9$ and d-PSS$_{35}$ were synthesized in deuterated form for use in neutron studies, and $(C_8D_8)_{(1-x) \, mol\%}(C_8D_7-SO_3H)_{x \, mol\%}$.

Differently charged polyelectrolyte solutions, typically 1 mg/mL, were prepared by dissolving accurately quantities of dry materials in a 2:1 (v:v) chloroform/methyl alcohol mixed solvent. In each experiment, a known volume of the solution was carefully added to the water surface in 5–10 μL increments, using a Hamilton micro-syringe. To ensure the complete evaporation of the solvent, a sufficient time (∼30 min) was allowed before the start of the measurements. Hysteresis was performed in the same manner as described earlier, but for four continuous cycles, each having the same rate for the compression and expansion cycle. Each expansion cycle was begun soon after the compression cycle. The stability of different polyelectrolyte monolayers with respect to time was studied by constantly observing the change in surface pressure for a period of nearly 4–5 h.

2.3. Neutron reflectivity

Specular neutron reflectivity was performed on a NG7 horizontal liquid reflectometer [23] at the Center for Neutron Research (National Institute of Standards and Technology, Gaithersburg) using a wavelength, λ of 4.76 Å. A mini Langmuir trough was mounted on the reflectometer so that in situ isotherms measurements could be made concurrently with the neutron measurements. The slit settings were adjusted so as to fix the resolution at a constant value of dq/q = 0.03. The horizontal slits were set at 30 mm. A one-dimensional position sensitive detector (PSD) having 255 channels oriented perpendicular to the sample surface enabled the specular intensity and an incoherent background scattering to be simultaneously recorded. Details of the NR experimental setup and data acquisition procedures have been described elsewhere [24–26].

3. Results and discussion

3.1. π–A isotherms

Phase information for Langmuir films can be obtained by an analysis of π–A isotherms where compressibility, phase transition, and stability of Langmuir films that are closely related to interactions between molecules can be characterized. π–A isotherms of random PSS copolymers with a variety of degrees of sulfonation are shown in Fig. 1. In general, we were able to observe a common plateau region in these phase isotherms, signifying that these PSS experience phase transitions upon compression. We first focused on determining whether the inception of a plateau or its collapse occurs at a different surface pressure for polymers with various degrees of sulfonation. Especially, a plateau is believed to signify phase transition related to solvation, submerging or packing of polymer chains.

PSS with 4 and 5% degrees of sulfonation show the highest plateau (∼45 mN/m) and collapse pressure (∼65 mN/m), indicating that they are highly compressible and aggregated at the collapse pressure due to strong hydrophobic interaction between PS monomers. On the other hand, PSS with between 6 and 16% sulfonation show a moderate plateau (∼30 mN/m) and collapse pressure (∼37 mN/m), where hydrophobic interactions are
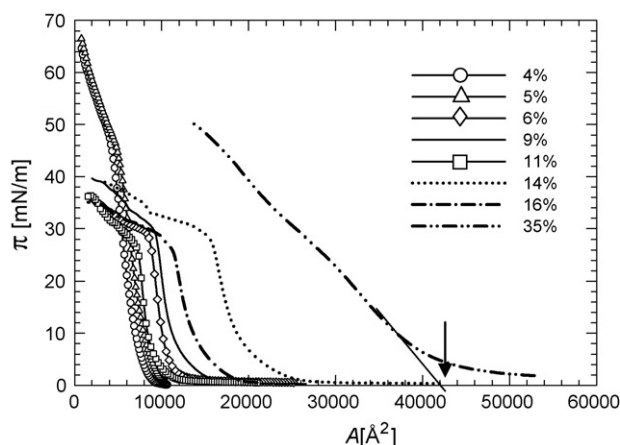
Fig. 1. Pressure–area per molecule (π–A) isotherms of PSS_x ($x = 4$–35%) at air/water interface. The arrow indicates the onset pressure of d-PSS_{35} in the isotherm.

counterbalanced by electrostatic interactions between negatively charged monomers.

For PSS with 35% degree of sulfonation, very weak plateau is shown in the range of 25–35 mN/m appeared in the isotherm and surface pressure increment upon compression is much less than any other polymer. It seems that a phase transition of PSS_{35} monolayer is slow down due to the electrostatic repulsion. Here we define an onset area indicated by arrow as a point where surface pressure start to increase in the isotherm. Even though PSS_{35} layer is compressed to three-fold from an onset area of $\sim$4200–1400 Å, compressed PSS_{35} layers do not reach neither a strong plateau nor collapse point while the other polymer does. This implies that highly stretched polymer chain of PSS_{35} on the water forms tethered brush-like structure under the water subphase upon compression. This will be proved by neutron reflectivity studies.

Therefore based on the isotherm analysis, behavior of the compressed monolayer can be categorized by three distinct regimes, referred to as *hydrophobic*, *ionomer*, and *polyelectrolyte*. This categorization is strongly dependent on the effect of charge, which appears to dictate the phase transition trend.
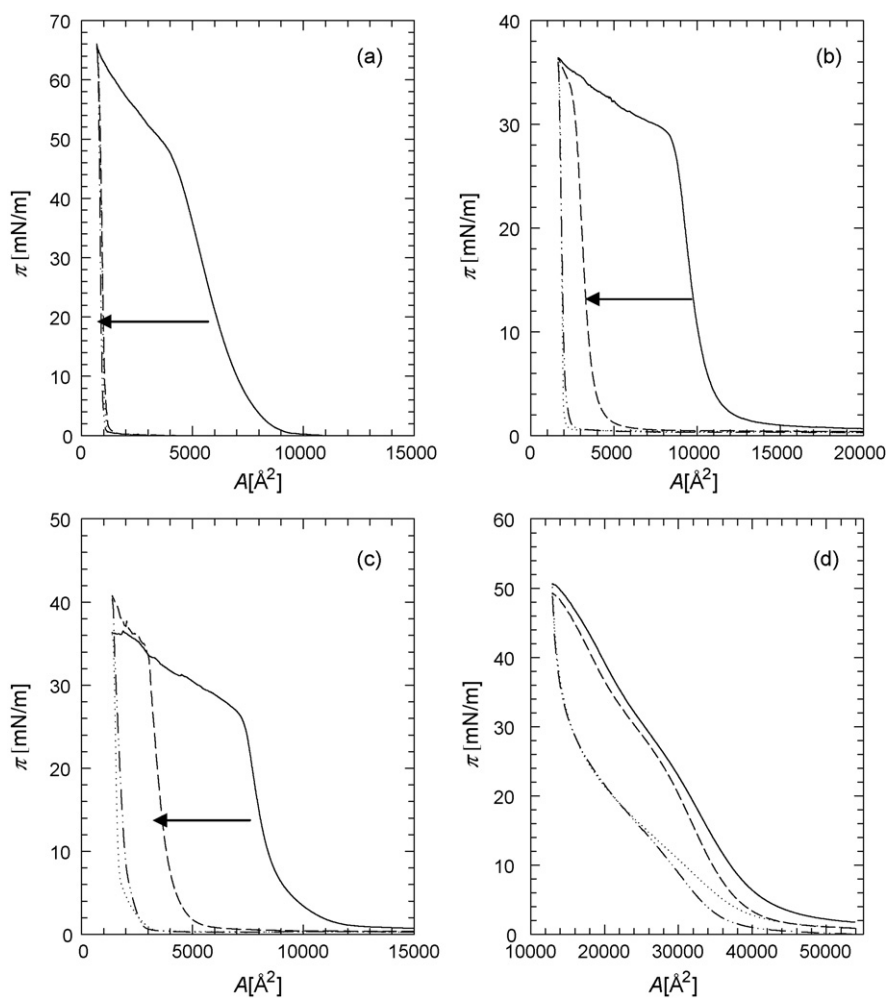

Fig. 2. Hysteresis effect of PSS_x monolayers: (a) PSS_4; (b) PSS_6; (c) PSS_{11}; (d) d-PSS_{35}. The compression and expansion isotherms are denoted as follows: (—) first compression, ($\cdots$) first expansion, (— — —) second compression, and (— · · —) second expansion. The arrows indicate hysteresis in the isotherms between the first compression and second compression.

Together with the effect of charge, the compositional factor in PSS imparts an equal contribution to its phase isotherms.

3.2. Hysteresis in the isotherms

In order to determine the stability of the monolayer and deduce information concerning the relative strength between hydrophobic and electrostatic interactions for differently charged PSSs, a hysteresis study is necessary. For the hysteresis measurements, we performed two compression and expansion cycles for the same monolayer. Once the monolayer was compressed to a certain surface pressure and then suddenly released without any delay. We measured the hysteresis for a complete range of PSS with 4–35% sulfonation, and four cases are displayed in Fig. 2.

A high hysteresis was observed for the low charged PSS 4% in Fig. 2a. After the first compression compressed films are unable to expand again even though the pressure is released (indicated by an arrow). Because of strong hydrophobic interaction between the monomers, irreversible aggregation occurs upon compression. A rigid and slightly white-colored aggregated layer after the first compression was observed with the naked eye. This behavior can be categorized into a *hydrophobic* regime. As the degree of sulfonation increases, compressed films were expanded somewhat, i.e., less hysteretic as shown in Fig. 2b and c. For second compression–expansion cycle, however, hysteretic behaviors become similar to the case in Fig. 2a. It is thought that once uncharged monomers from the first compression aggregates into cluster forms, repulsive interaction between the charged monomers around the clusters is insufficient for overcoming a strong hydrophobic interaction between them. This is somewhat different from the first case so that it can be categorized into an *ionomer* regime.

PSS with 35% shows almost negligible hysteretic behavior, at least in the first compression–expansion cycle, as shown in Fig. 2d. The improvement in reversibility was due to the dominance of electrostatic interactions over hydrophobic interactions. It is now clear that the amount of charge in a polymer chain has a strong influence on the reversibility. This behavior is also different from the former two cases so that it can be categorized by a *polyelectrolyte* regime.

3.3. In situ neutron reflectivity

In order to find whether polymer chains with ionized ions are submerged in water, specular neutron reflectivity (NR) was performed. NR data are very sensitive to the structure of the deuterated chains, which are in contact with the lower SLD medium, the water subphase (SLD $= -5.6 \times 10^{-7}\,\text{Å}^{-2}$).

Fig. 3a shows the neutron specular reflectivity of perdeuterated PSS$_9$ Langmuir films at two different surface pressures. The solid lines together with the symbols are the fits obtained for the corresponding SLD profiles, which are shown in Fig. 3b. Each data set in Fig. 3 shows a unique interference fringe, which contains only the form factor for the film without a q^{-4} decay. Fits to the reflectivity data (solid lines) were obtained from a two layer model as shown in Fig. 3b, consisting of an upper layer
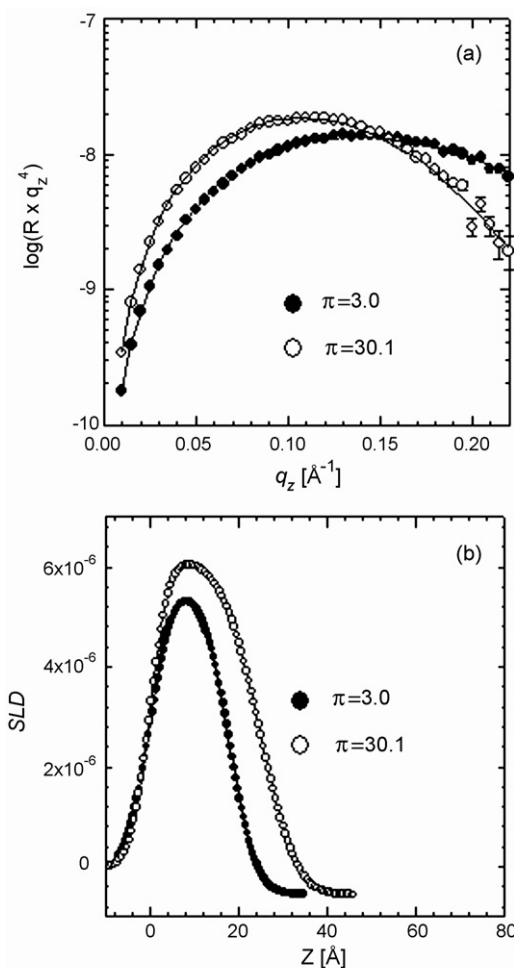

Fig. 3. (a) Neutron reflectivity data for a d-PSS$_9$ monolayer at the air/water interface. The solid lines through the data are the best fits, and (b) are the corresponding SLD profiles obtained from the fits. The x-axis z is taken from air.

of floating d-PSS hemi-micelles on the subphase surface and a lower layer of sulfonated corona chains submerged in the subphase medium. The y-axis represents a SLD, the real part of the refractive index (n). Note that the lower layer is not noticeable in this profile, because most of the chains remain near water surface.

The Parratt algorithm was applied for the fitting routine [27]. Details of this model, experimental techniques, and theoretical formulae can be found in previous papers [9]. The parameters, including thickness (d), roughness (σ), and SLD obtained from the fits are summarized in Table 2. Each layer of polymer chain was well fitted with the general Gaussian distribution function for each interface used in this model of an independent layer.

At low pressure, PSS$_9$ layer formed a 18 Å thick layer and then by increasing the surface pressure to 30.0 mN/m (close to the plateau in the isotherm shown in Fig. 1) becomes 27 Å. It is noted that the increased layer thickness is mainly due to a increase in the upper layer, indicating that submersion of the charged monomer are not significant even after full compression.

Table 2
Fitting parameters from NR of for d-PSS$_9$ and d-PSS$_{35}$ at the air/water interface

π (mN/m)	t_1 (Å)	t_2 (Å)	σ_1 (Å)	σ_2 (Å)	σ_3 (Å)	SLD$_1$ (10^{-6} Å^{-2})	SLD$_2$ (10^{-6} Å^{-2})
Fig. 3							
3.0	16	2	4.0	7.5	4.4	5.6	4.5
30.1	22	5	3.4	6.5	5.8	6.1	2.9
Fig. 4							
5.1	8	2	4.8	12.7	4.3	5.6	4.2
22.3	11	2	5.1	18.2	4.4	5.9	4.8
36.0	11	3	6.1	18.0	4.5	6.0	6.2
	13	–	4.4	–	–	5.6	–
48.0				$^a f(z) = A \times 10^{-6}(1 - (z/B)^2)^C$, $A = 0.64$, $B = 60$, $C = 1$			

^{a} The SLD profile of the second layer was obtained from the brush density profile described in Ref. [28].

Fig. 4a shows NR data obtained for d-PSS$_{35}$. The solid lines in Fig. 4a are the fits obtained with the model shown in Fig. 4b. At low π, total layer thickness of 10 Å is considerably thinner than that of PSS$_9$. This may be because the highly charged chains were fully stretched and flattened at the air/water interface. As π increases, the total film thickness increases progressively to 14 Å for $\pi = 36$ mN/m. Interestingly, at $\pi = 48$ mN/m, NR
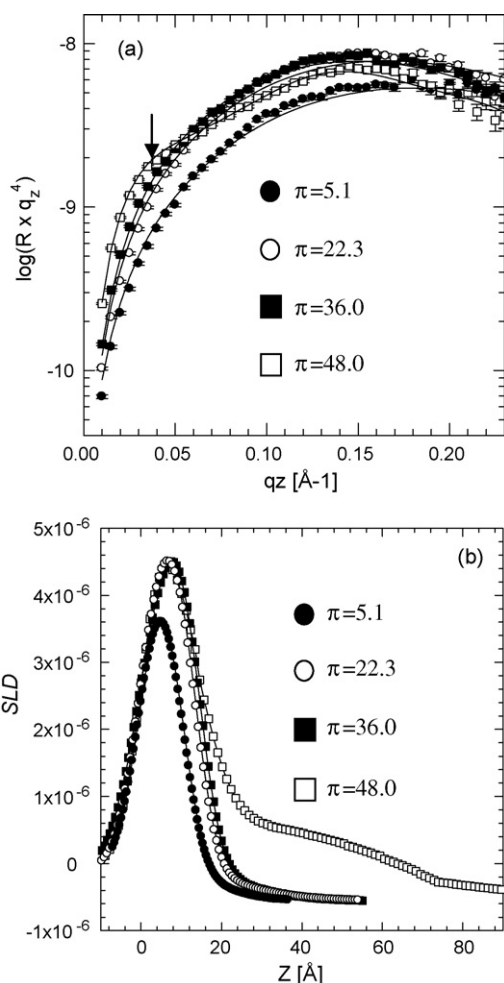

Fig. 4. (a) Neutron reflectivity data of d-PSS$_{35}$ monolayer spread at the air/water interface. The solid lines through the data are the best fits. An arrow indicates the presence of diffused chains submerged into the water subphase and (b) is the corresponding SLD profiles obtained from the fits.

profile in Fig. 4a shows that the oscillation curve develops a kink at q_z −0.04 Å^{-1} (marked by the arrow). The profile fits only to a parabolic bottom layer with layer thickness of approximately > 60 Å, with the parabolic layer profile given by SLD$_2(1 - (z/d_2)^2)$, where SLD$_2$ and d_2 are the scattering length density at the interface of the upper and bottom layer, respectively, and d_2 is the thickness cutoff for the bottom layer [28].

Therefore the bottom layer seems fully extended into the water and the upper layer remains almost constant, functioning as floating points on the water surface. This transition might occur at the plateau in π–A isotherm as shown in Fig. 1. Moreover, the transition is in fact reversible and reproducible, as observed in the hysteresis curves shown in Fig. 2d.

In summary partially solvated PSS chains with sulfonation higher than 35% are reversibly submerged into the water subphase with increasing surface pressure at the air/water interface. To our knowledge, this reversible brush-transition of polyelectrolytes at an air/water interface has not previously been observed.

4. Conclusion

Langmuir monolayers of randomly charged PSS$_x$ with various degrees of sulfonation (x) ranging from 4 up to 35% were studied. The randomly charged PSS were found to be amphiphilic and stable at the air/water interface. We observed reversible contraction and stretching of polyelectrolytes with ionic contents $x \geq 35\%$ at the air/water interface using in situ NR measurements. We could finally categorize those polyelectrolytes into three different regimes, *hydrophobic* (<5%), *ionomer* (6–16%), and *polyelectrolyte* ($\geq$35%) as a function of the degree of sulfonation.

Acknowledgements

References

[1] S. Schlick (Ed.), Ionomers; characterization, theory, and applications, CRC Press, Boca Raton, 1996.

[2] C.G. Gebelein, Biomimetic Polymers, Plenum Press, New York, 1990.

[3] P. Pincus, Macromolecules 24 (1991) 2912.

[4] G. Decher, Science 277 (1997) 1232.

[5] S.K. Tripathy, J. Kumar, S.H. Lee, Langmuir 17 (2001) 3491.

[6] A.C. Balazs, C. Singh, E. Zhulina, Macromolecules 31 (1998) 6369.

[7] G. Ladam, P. Schaaf, F.J.G. Cuisinier, J.C. Voegel, Langmuir 17 (2001) 878.

[8] E.P.K. Currie, A.B. Sievel, G.J. Fleer, M.A.C. Stuart, Langmuir 16 (2000) 8324.

[9] K. Shin, M.H. Rafailovich, J. Sokolov, D.M. Chang, J.K. Cox, R.B. Lennox, A. Eisenberg, A. Gibaud, J. Huang, S.L. Hsu, S.K. Satija, Langmuir 17 (2001) 4955.

[10] Y.V. Lyatskaya, F.A.M. Leermakers, G.J. Fleer, E.B. Zhulina, T.M. Birshtein, Macromolecules 28 (1995) 3562.

[11] M. Beisalski, J. Ruhe, D. Johannsmann, J. Chem. Phys. 111 (1999) 7029.

[12] S.W. An, P.N. Thirtle, R.K. Thomas, F.L. Baines, N.C. Billingham, S.P. Armes, J. Penfold, Macromolecules 32 (1999) 2731.

[13] X. Chatellier, J.F. Joanny, J. Phys. II France 6 (1996) 1669.

[14] C. Poncet, F. Tiberg, R. Audebert, Langmuir 14 (1998) 1697.

[15] M.F. Durstock, M.F. Rubner, Langmuir 17 (2001) 7865.

[16] G.J. Fleer, M.A. Cohen Stuart, J.M.H.M. Scheutjens, T. Cosgrove, B. Vincent, Polymer at Interfaces, Chapman and Hall, London, 1993.

[17] S.Y. Park, C.J. Barrett, M.F. Rubner, A.M. Mayes, Macromolecules 34 (2001) 3384.

[18] J. Li, W. Zhao, J. Quinn, M.H. Rafailovich, J. Sokolov, R.B. Lennox, A. Eisenberg, X.Z. Wu, M.W. Kim, S.K. Sinha, M. Tolan, Langmuir 11 (1995) 1785.

[19] J. Zhu, A. Eisenberg, R.B. Lennox, J. Am. Chem. Soc. 113 (1991) 5583.

[20] H. Yim, M. Kent, A. Matheson, R. Ivkov, S. Satija, J. Majewski, G.S. Smith, Macromolecules 33 (2000) 6126.

[21] O. Theodoly, R. Ober, C.E. Williams, Eur. Phys. J. E 5 (2001) 51.

[22] H.S. Makowski, R.D. Lundberg, G.H. Singhal, US Patent: 3,870,841, EXXON Research and Engineering Company (1975).

[23] P.J. Flory, Principles of Polymer Chemistry, Cornell Univ. Press, Ithaca, New York, 1971.

[24] J.F. Ankner, C.F. Majkzak, S.K. Satija, J. Res. Natl. Inst. Stand. Technol. 98 (1993) 47.

[25] T.P. Russell, Mater. Sci. Rep. 5 (1990) 171.

[26] K. Shin, M.H. Rafialovich, J. Sokolov, D. Gersappe, M.W. Kim, S.K. Satija, D. Nguyen, D. Xu, N.-L. Yang, A. Eisenberg, Langmuir 17 (2001) 6675.

[27] L.G. Parratt, Phys. Rev. 95 (1954) 359.

[28] A. Karim, S.K. Satija, J.F. Douglas, J.F. Ankner, L.J. Fetters, Phys. Rev. Lett. 73 (1994) 3407.